Loss of Excitation Detection in Doubly Fed Induction Generator by Voltage and Reactive Power Rate

M. J. Abbasi* and H. Yaghobi*(C.A.)

Abstract: The doubly fed induction generator (DFIG) is one of the most popular technologies used in wind power systems. With the growing use of DFIGs and increasing power system dependence on them in recent years, protecting of these generators against internal faults is more considered. Loss of excitation (LOE) event is among the most frequent failures in electric generators. However, LOE detection studies heretofore were usually confined to synchronous generators. Common LOE detection methods are based on impedance trajectory which makes the system slow and also prone to interpret a stable power swing (SPS) as a LOE fault. This paper suggests a new method to detect the LOE based on the measured variables from the DFIG terminal. In this combined method for LOE detection, the rate of change of both the terminal voltage and the output reactive power are utilized and for SPS detection, the fast Fourier transform (FFT) analysis of the output instantaneous active power has been used. The performance of the proposed method was evaluated using Matlab/Simulink interface for various power capacities and operating conditions. The results proved the method's quickness, simplicity and security.

1. Introduction

The wind power has received support by the governments of many countries and so has promoted a lot. Particularly in Europe, where shallow-water and offshore wind resources are multitudinous, large-scale offshore wind farms are developed. By 2020 in Europe, it is forecasted that 20% of power consumed will be generated by renewable resources [1]. Over the years in wind energy conversion systems, various types of generators and associated interfaces have been widely employed. As the operation speed has changed from nearly constant to variable speeds, Doubly Fed Induction Generator (DFIG) has got to be widely employed in many present day wind farms for its higher performance in comparison to the ordinary squirrel cage induction generators [2]. Like other electrical generators, DFIGs may also be affected by the electromechanical failures. Therefore, early detection of faults in the initial stages is necessary to prevent spreading faults and damage to the machine and the power system. Studies on the fault rates of wind turbine induction generators, including the DFIGs, demonstrated that between 31% of generators' faults are related to the rotor [3]. As

noted above, loss of excitation (LOE) of the DFIG is a probable fault which is essential to be diagnosed early. Such a fault could be due to various reasons, such as a short circuit or open circuit in the excitation circuit, failure in converters or other power electronic equipment. Subsequently, because of temperature rise, the LOE leads to damage to the rotor and stator windings, end-core area and also the imposition of stresses on the rotor, shaft and other mechanical parts. Another consequence of LOE is absorbing the reactive power by the DFIG, voltage drop and possible damages to power system equipment and loads. The early detection of LOE is an important factor to prevent these damages or at least to minimize them [4]-[6].

Most of the existing LOE detection methods have been proposed for synchronous generators in which impedance based methods are often employed [7-9]. The major disadvantage of impedance based methods, apart from the long time needed for LOE detection, is the possibility of incorrect operation during the stable power swing (SPS). A time delay is commonly added to tackle the problem, however the resulting slow-down of the relay response and prolongation of fault conditions lead to some undesired consequences on the machine and the network. The next category involves a neural network based methods [10] and [11] that are not much interested because of their need for numerous training data and massive calculations involved. In another method [5], instead of direct application of impedance, a fuzzy inference mechanism is applied to the impedance and voltage, and consequently the

impedance relay function in SPS detection is promoted; even though the relay response speed is not satisfactory enough. In some other method [12-15], the flux measurement of the machine is proposed as the solution which significantly promotes the speed and security; the used sensor may cause damage to the machine however.

In the latest research, a novel technique based on the derivatives of terminal voltage and output reactive power has been presented [6]. In this reference, in order to evaluate the performance of the proposed technique, some comprehensive studies are performed for different conditions that demonstrate the proposed method operates more quickly. Nevertheless, there are reports, uttering the possibility of misinterpreting SPS for LOE, in heavy loading conditions of machine under a leading power factor [11-14]. In this reference also, the time delay solution is proposed to overcome the problem. Accordingly, the majority of methods have so far utilized the time delay.

On the other hand, virtually, few research works has been reported in order to detect LOE in the DFIG. For instance, in [4] the LOE simulation in DFIG is performed and the effects of this fault on the DFIG output characteristics are discussed as the first step. In the following, the authors have proposed the utilization of terminal voltage and output reactive power to detect the LOE. For fault detection, then, the neural network based method is suggested. As stated earlier, these methods require considerable amount of training data for all possible conditions. LOE fault in DFIG and its effects on fault ride through (FRT) capability of DFIG are discussed in [16] and [17]. Terminal voltage and output reactive power reduction are emphasized as the most important consequences of LOE in DFIG in the recent references.

Therefore, the purpose of this research is to present a suitable technique for LOE detection in DFIG that can quickly identify SPS. This paper suggests a new method to detect the LOE, based on the measured variables from the DFIG terminal. In this combined method for LOE detection, the rate of change of both the terminal voltage and the output reactive power is employed, while for SPS detection, the fast Fourier transform (FFT) analysis of the output instantaneous active power has been used. The method requires two threshold values. Furthermore, the time delay associated with the calculation of FFT should be considered. This paper is organized as the following: the concept of LOE in the DFIG is explained in section 2, in section 3, the new method is presented for LOE and SPS detection. In section 4, comprehensive studies using the new method are applied and section 5, are dedicated to a conclusion.

2. Concept of LOE in DFIG

In this section, first the performance of the DFIG is investigated and the governing equations of the DFIG voltage, active and reactive powers for healthy state are demonstrated, then a mathematical expression for LOE fault is presented.

2.1. DFIG Operation and Control Model

The DFIG structure consists of a wound rotor induction generator in which the rotor is fed by a back to back converter and the stator is directly connected to the network. The control system of DFIG converters is shown in Fig. 1 (a). The converter adjusts voltage and frequency of the rotor. By adjusting the frequency of the rotor, the stator frequency remains constant (60 Hz, here) in different modes of operation, and by regulating the voltage of the rotor, the stator voltage is regulated according to a predetermined value. Setting the frequency of the rotor allows the machine to operate at variable speeds (about 0.7 to 1.3, times base speed) which is unlike the squirrel cage induction generator which has an almost constant speed (one or two percent change from base speed). This causes less mechanical stress on the turbine and especially the driving part of it [18]. Vector control (VC) method is used to control the grid-side converter (GSC) and rotor-side converter (RSC). Controlling the active and reactive power of DFIG is separately performed by VC of RSC, thus achieving the regulatory power factor is possible. Also, VC of GSC in addition to support the DC link voltage can control the reactive power exchanged between the GSC and the power grid [4], [19].

2. 2. Equations of d-q Rotating Reference Frame for Healthy Machine

The dynamic model of the DFIG in d-q variables is stated with the following equations. L_m is the magnetizing inductance, L_s and L_r are the stator and rotor inductances, $L_s=L_m+L_{ls}$, $L_r=L_m+L_{lr}$. L_{ls} and L_{lr} are stator and rotor leakage inductance, respectively. The flux linkage equations can be expressed as follows [20]:

$$\begin{aligned}
\Psi_{ds} &= L_s\, i_{ds} + L_m\, i_{dr} \\
\Psi_{qs} &= L_s\, i_{qs} + L_m\, i_{qr} \\
\Psi_{dr} &= L_r\, i_{dr} + L_m\, i_{ds} \\
\Psi_{qr} &= L_r\, i_{qr} + L_m\, i_{qs}
\end{aligned} \tag{1}$$

where, subscripts s and r, represent the variables of stator circuit and rotor circuit, respectively. Also, the voltage equations of the machine can be expressed as follows [20]:

$$\begin{aligned}
u_{ds} &= R_s\, i_{ds} + p\,\Psi_{ds} - \omega\Psi_{qs} \\
u_{qs} &= R_s\, i_{qs} + p\,\Psi_{qs} + \omega\Psi_{ds} \\
u_{dr} &= R_r\, i_{dr} + p\,\Psi_{dr} - (\omega-\omega_r)\Psi_{qr} \\
u_{qr} &= R_r\, i_{qr} + p\,\Psi_{qr} + (\omega-\omega_r)\Psi_{dr}
\end{aligned} \tag{2}$$

where, ω and ωr are synchronous speed and rotor angular speed, respectively. Also, p represents the operator d/dt. By using the below equations, active and reactive power at the stator terminal can be calculated [4]:

$$P_s = \frac{3}{2}u_{qs}\,i_{qs} = -\frac{3}{2}u_s\frac{L_m}{L_s}i_{qr}$$

$$Q_s = \frac{3}{2}u_{qs}\,i_{ds} = \frac{3u_s}{2L_s}\left(\Psi_s - L_m\,i_{dr}\right)$$
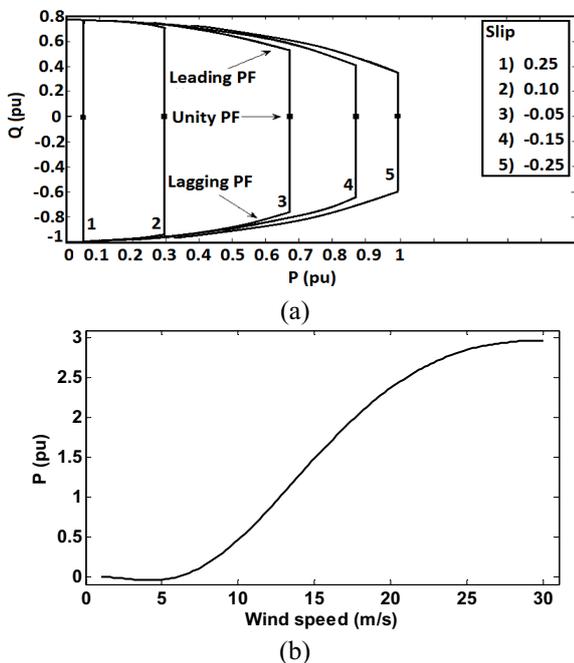
(3)

(a)

(b)

Fig. 2. (a) DFIG power capability curve in per units [24]. (b) Wind turbine output power versus wind speed.

2. 3. LOE Fault

When a DFIG loses its excitation, the rotor current can be written as follows:

$$i_{dr} = 0,\ i_{qr} = 0$$

(4)

Using (1), (2), and (4) the governing equations of the DFIG voltages during LOE fault can be determined. Also, using (3) and (4), power equations are obtained. As a result, these equations can be solved to calculate terminal voltage and output power after LOE, using a suitable numerical technique.

3. Proposed Method

3. 1. Simulation Model

Commonly, a big wind farm in a power system contains tens or hundreds of single wind turbines. There is no mutual interaction among wind turbines in a wind farm if the converters are well-regulated, and the issue is not at all depended to the power system conditions [21]. One or several independent DFIG may exist in a local network or a micro-grid [4]. Each of them is equivalent to a generator connected to the network, which is frequently used as a test system in recent LOE detection studies [5], [6]. Considering all the above mentioned points, to simulate the LOE fault, a DFIG connected to the network is exploited herein. The simulation model shown in Figs. 1 (a) and 1 (b) is provided using Matlab/Simulink [22], [23]. The complete view of the simulated system in the Simulink is presented in Fig. 1 (c). Through a step-up transformer, the DFIG is connected to two parallel lines. Thermal limits for each line and an increase of the reliability of the systems are two main reasons for the parallel lines to be utilized in power systems [21]. A 25/120 kV transformer then, connects the intended system to the power grid. Power capability curve of the DFIG is shown in Fig. 2 (a). In Fig. 2 (b) is shown the output power versus wind speed characteristic of the wind turbine, which is used in the simulation model. For details about the simulation model, refer to the appendix.

3. 2. LOE detection

In order to diagnose LOE fault in DFIG using the simulation model, Fig. 1 (b), a three phase short circuit was applied to the excitation winding terminal of the DFIG [4]-[6], in 3rd second. After the occurrence of the LOE, DFIG output parameters change as shown in Fig. 3 (a). Among these parameters, terminal voltage and current are per units of DFIG nominal values which are listed in the Appendix. Changes of terminal voltage and current are seen in Fig. 3 (a). Accordingly, after the LOE event, the terminal voltage would decrease by only some percent, while the current increases more than fourfold. According to Fig. 3 (a), also the output active power decreases significantly. After the LOE event, the active power decreases to near zero and DFIG absorbs the reactive power from the network, which makes a voltage drop in the network. As noted above, following the LOE event, terminal voltage and output reactive power will decrease. The proposed method uses the same behavior of voltage and reactive power to identify the LOE. For proper visibility of the voltage variations, RMS value of the voltage (Vt) has been used. Fig. 3 (b) shows the output reactive power and the RMS value of the terminal voltage.
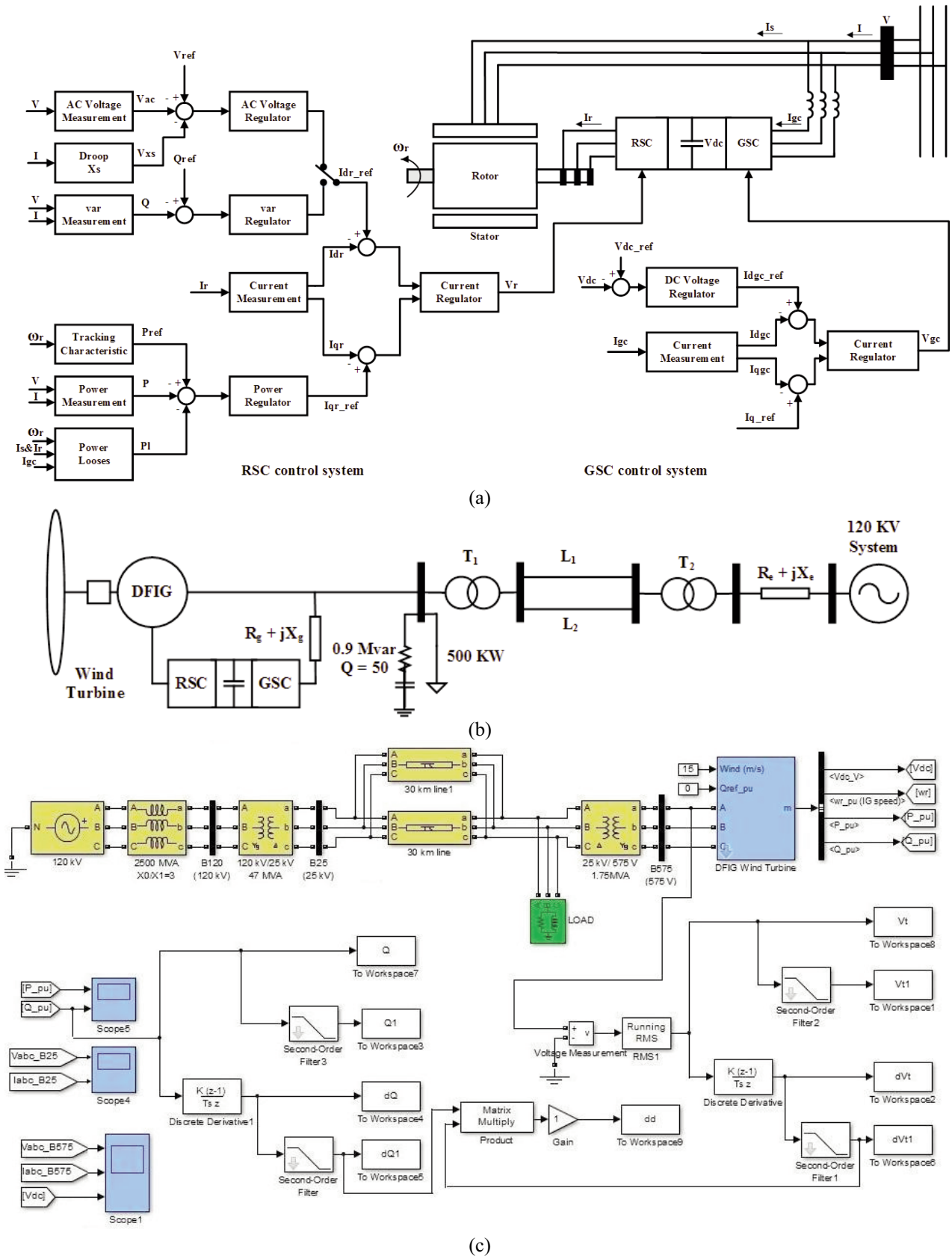
Fig. 1. (a) Control systems for rotor-side and grid-side converters [22]. (b) Single-line diagram of the DFIG connected to the network [23]. (c) Complete view of the simulated system in the Simulink.

As is evident in Fig. 3 (b), after the LOE event, terminal voltage gradually decreases. Fig. 3 (b) also reveals that in the same conditions, the reduction of reactive power is more severe, although both waveforms have the same behavior.

The new technique is based on the behavior of the generator terminal voltage and output reactive power. By multiplying the rate of change of these two parameters, an index for identifying the LOE event has been obtained.
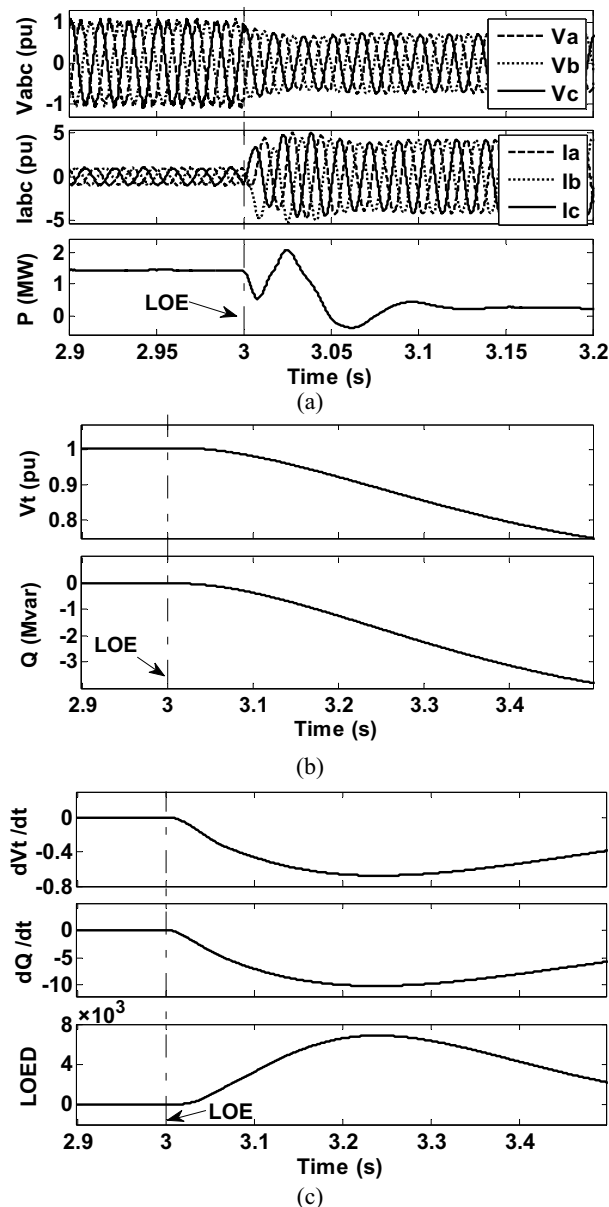

Fig. 3. (a) DFIG terminal voltage and current and output active power after LOE. (b) RMS value of terminal voltage and output reactive power for LOE event. (c) Derivatives of terminal voltage and output reactive power and the LOED for LOE event.

Fig. 3 (c) shows these parameters for LOE event. As seen in Fig. 3 (c), terminal voltage and reactive power both have negative derivatives after the LOE event, but it is more significant for reactive power. Also Fig. 3 (c) shows the multiplication of derivatives of terminal voltage and output reactive power is positive, because these two values are negative. In fact, this is a loss of excitation detector (LOED) for DFIG [6] which is obtained according to (5).

$$LOED = C \times \frac{dV_t}{dt} \times \frac{dQ}{dt} \qquad (5)$$

where Vt and Q are terminal voltage and output reactive power values, respectively. Also, d/dt is derivative operator and C is a constant (namely 103) which is used for better visibility of LOED.

The LOE is diagnosed when the LOED exceeds a predetermined value. In fact, this predetermined value is an actuator (A) value for LOE relay, which is determined according to the conditions of the generator and power system such as generator rated power, generator output power before fault and power system configuration.

3. 3. Strategy of SPS Detection

One of the important problems about LOE relays is the risk of maloperation during the SPS. In order to investigate SPS effect on the performance of the proposed method in this paper, a three-phase short circuit fault in one of the transmission lines has been considered which makes severe voltage drop at the DFIG terminal [5], [6]. The SPS occurs in the 8th second and its duration is assumed to be 200 ms. For a 1.5 MW DFIG, Fig. 4 shows the terminal voltage, output reactive power, LOED changes and output instantaneous active power for the SPS event. Fig. 4 clearly shows that after the fault occurrence and during the fault condition, the terminal voltage decreases and the output reactive power increases. Also in this time interval, the LOED has a negative value. Afterwards, the SPS starts with fault clearing. In stable power swing condition, the mentioned process of the terminal voltage and reactive power continues for moments and then after a while starts to recover. As shown in Fig. 4, the computed LOED has a positive value in a short time interval during the SPS and it predisposes the LOE relay to maloperation. To overcome this problem in this paper, an efficient solution has been used. The proposed solution utilizes the FFT analysis of output instantaneous three-phase active power to identify the SPS as explained in the following. Meanwhile, for brevity, the output instantaneous three-phase active power will be called output active power henceforth.

In a power system, events such as a short circuit in transmission lines, sudden change in loads or system con-

figuration, etc. may lead to the SPS condition [4]-[6]. So, the generator output active power begins to oscillate. Identifying the dominant frequency of these power swings is used as a strategy for SPS detection in the proposed method. The authors in [25] have considered that there are
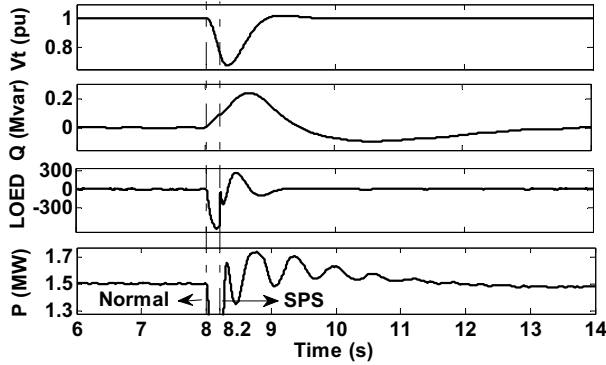

Fig. 4. Terminal voltage, output reactive power, the calculated LOED and output instantaneous active power for the SPS event.

two sources with various frequencies for SPS condition, which are close to the main frequency of the power system.
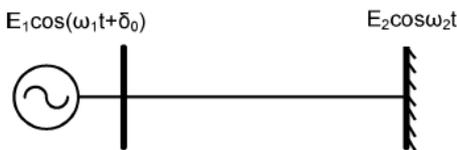
During the SPS, the difference between these two fre-

Fig. 5. Power system with two frequencies during the SPS [25].

quencies is very small. Accordingly, the power system during the SPS is considered to be equivalent to Fig. 5.

Also, in [25] it has been established that during the SPS, the output active power oscillates at the low frequency (the frequency difference between the two sources), which is the specific frequency in the range of 0.3-7 Hz. Fig. 4 shows the output active power for the SPS event. As could be seen, in the SPS time interval, the output active power oscillates with low frequency. The result is, if the FFT is performed on the output active power, the low frequency (here 0.3-7 Hz) components will take a significant value during the SPS, whereas it decreases to a low value after the LOE fault. Accordingly, this feature as a stable power swing detector (SPSD) has been used as follows:

$$SPSD = \sum_{i=0.3}^{7} \text{FFT coefficients of } (i)\text{ Hz}$$
component, step for i=0.1 (6)

The calculated SPSD value is compared with a predetermined value, which is a blocker (B) value for LOE relay. If the SPSD exceeds the B value, the event is known as the SPS and the LOE relay is blocked.
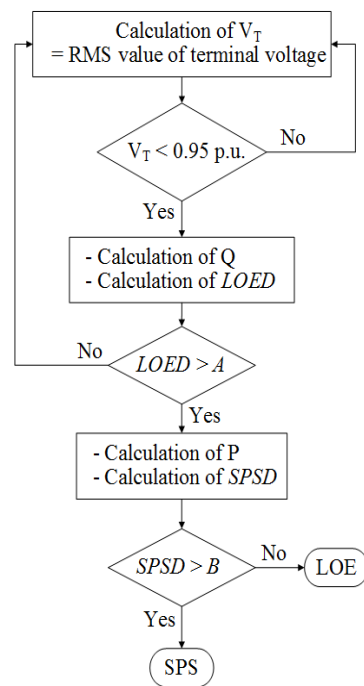

Fig. 6. Proposed flowchart for LOE relay of DFIG.

3. 4. A Basic Algorithm for the Proposed Method

The general logic of the proposed method is shown as a flowchart in Fig. 6, which is a combination of LOED and SPSD strategies. When the terminal voltage drops to less than 0.95 p.u., the LOED index is calculated using the derivatives of the terminal voltage and the output reactive power. In case the calculated LOED exceeds the A value, it should be examined whether it is actually an LOE event or not.

To make that happen, the algorithm computes the DFIG output active power using the sampled voltages and currents and by applying the FFT on the output, the frequency components within a power cycle are extracted.

This method does not require a high sampling frequency and can operate at frequencies common in digital protective relays [25]. With a sampling frequency of 1 kHz and for a 60 Hz power system, the data window (or the power cycle) is 16.67 ms that is close to 17 samples. Contrary the delay time elapsed in conventional LOE relay; this is a short time for SPS detection and accelerates the method significantly. The SPSD is computed in every power cycle (after Vt <0.95 p.u. and LOED>A) and when exceeds the B value, an SPS is detected. Whenever the calculated LOED exceeds the A value, while the calculated SPSD remains below the B value, a LOE event is detected.

4. Performance Evaluation

Some extensive simulations considering different DFIG capacities and various loading conditions were carried out. The results of these simulations are organized in

Table 1. Loading point of DFIG

Loading		Slip	Wind speed for turbine	DFIG operational state
No.	P + jQ (p.u.)			
1	0.05 + j0.80		Cut-in	
2	0.05 - j0.01	25.26		
3	0.05 - j0.30			
4	0.25 + j0.20			
5	0.25 - j0.01	11.50		
6	0.25 - j0.60			Sub synchronous
7	0.30 + j0.55		Normal-low	
8	0.30 - j0.01	9.47		
9	0.30 - j0.20			
10	0.50 + j0.63			
11	0.50 - j0.01	1.33		
12	0.50 - j0.80			
13	0.75 + j0.49			
14	0.75 - j0.04	-9.28		
15	0.75 - j0.65		Normal-high	
16	0.90 + j0.33			Super synchronous
17	0.90 - j0.04	-17.11		
18	0.90 - j0.20			
19	1.00 - j0.05	-25.14	Cut-out	

Table 2. Chosen Loading point for targeted studies Scenario

Scenario No.	Load level	Power factor	P + jQ (p.u.)
1	Light	Lagging	0.25 + j0.20
2	Light	Unity	0.25 - j0.01
3	Light	Leading	0.30 - j0.20
4	Heavy	Lagging	0.90 + j0.33
5	Heavy	Unity	1.00 - j0.05
6	Heavy	Leading	0.75 - j0.65

this section to evaluate the performance of the proposed LOE relay. During the investigations also, the appropriate values for defined threshold variables (A and B) in the proposed algorithm, have been obtained. In fact, based on the worst conditions, the setting of the threshold values should be defined i.e. LOE fault with a leading power factor condition and for the longest period of the power swing that can be expected (the frequency of 0.3 Hz)

The selected test machines are four DFIGs with capacities ranging from 1.5 MW to 3 MW. In order to choose the DFIGs loading points, the DFIG power capability curve and the wind turbine power characteristic have been used that are illustrated in Figs. 2 (a) and 1 (b), respectively. The given capability curves in Fig. 2 (a), are for wind speed from cut-in speed with 0.25 slip to cut-out speed with -0.25 slip [24]. Considering the power output versus the wind speed and the power conversion of the turbine, the capability curve for the DFIG was used and operational points were extracted. Accordingly, the loading points in per units, used to test the proposed method, are listed in Table 1 where to review the performance of all modes of DFIGs' operations, 19 loading points have been considered in different conditions. These operational points on the DFIGs will be capable to happen by changing the wind speed and settings the reactive power. With the aim of carrying out the comprehensive and inferable simulations a number of loading points presented in Table 1, based on the power factor and load level have been arranged in Table 2. In the following, the strategy of LOE detection would be tested, as well as the performance of the proposed solution for discrimination between LOE and SPS by means of Matlab/Simulink simulations.

4. 1. Loss of Excitation

The performed simulations in previous section indicated that LOED has a large positive value after the LOE event. In order to test the effect of the DFIG size on LOED value, another simulation test has been performed considering four different sizes for the DFIG. The calculated LOED of 1.5, 2, 2.5 and 3 MW DFIGs at loading No. 14, for a LOE event in the 3rd second is shown in Fig. 7 (a). As the figure shows, the overall pattern of LOED changes after LOE occurrence for all the DFIG sizes is similar. However, increasing the size of DFIG is associated with growth in the amount of LOED. This is reasonable because during LOE, large DFIGs experience great changes in reactive power. Additionally, assuming the same network connection for all the DFIGs, the network is stronger for the smaller ones and as a result, the rate of terminal voltage changes is lower, implying lower LOED amplitude.

To study the effect of pre-fault loading conditions from the viewpoint of load level and power factor effects on the LOED value, according to scenarios shown in Table 2 several simulations were performed to a 1.5 MW DFIG.

Figs. 7 (b) and 7 (c) illustrate the computed LOED for light and heavy loadings, including scenarios 1 to 3 and 4 to 6, respectively. Both Figs. 7 (b) and 7 (c) clearly show that the calculated LOED has a lower value in leading power factor. From these results it can be easily realized that the pre-fault loading of the DFIG with a leading power factor leads to a lower peak of LOED.
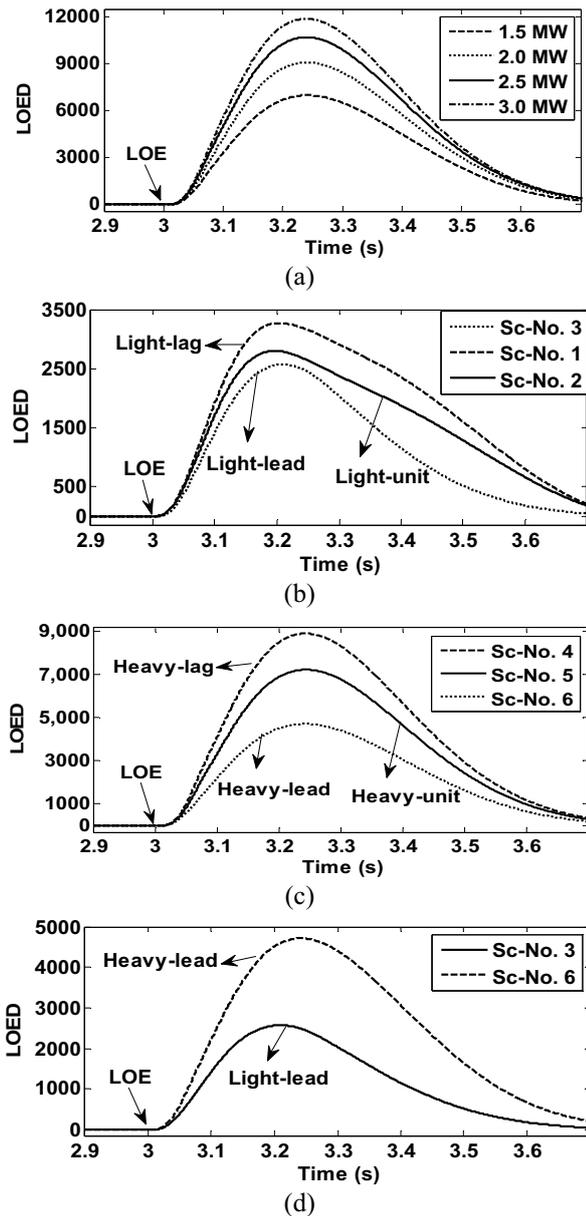
Also, the comparison between the calculated LOED

for scenarios 3 and 6 in Fig. 7 (d) shows that light load leads to a lower LOED. Finally, it can be concluded from the recent discussion that the least LOED amplitude belongs to the smaller DFIG that operates at the lightest possible loading under a leading power factor. Accordingly, the appropriate value of A was determined to be 100.

4. 2. Stable Power Swing

To ensure performance of the proposed SPS detection strategy, a series of simulation results for different DFIG sizes and various loading scenarios are illustrated in this section. As shown in Fig. 8 (a), the calculated LOEDs of all DFIG sizes during SPS, have the same behavior and exceed the set threshold. To distinguish that from the LOE condition, SPSD index should be calculated. The FFT coefficients of the output active power are measured herein as some percentage of the fundamental frequency coefficient. For instance, Fig. 8 (c) shows the FFT coefficients
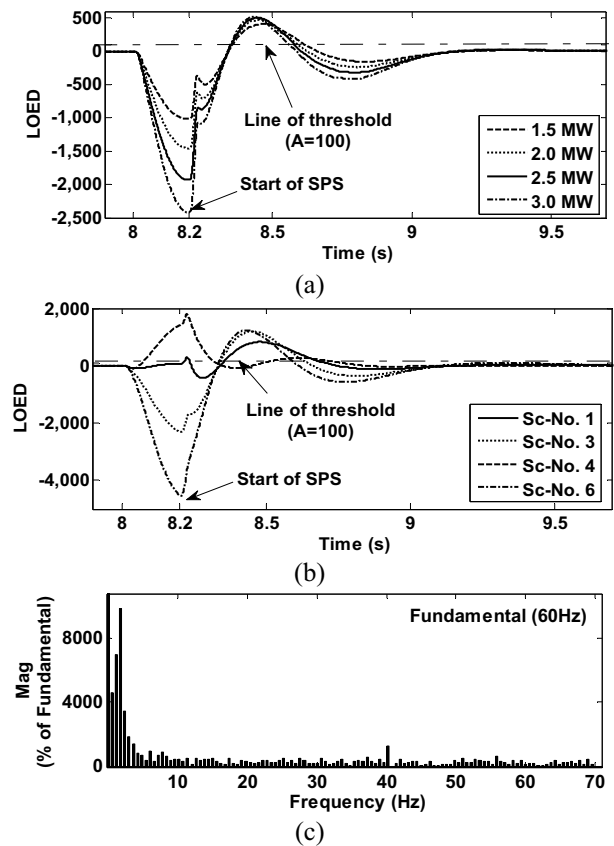

Fig. 7. (a) Calculated LOED of four DFIGs (1.5, 2, 2.5 and 3 MW) at loading No. 14. (b) Calculated LOED of a 1.5 MW DFIG for light loadings, including scenarios 1, 2 and 3. (c) For heavy loadings, including scenarios 4, 5 and 6. (d) LOED comparison for scenarios 3 and 6 after LOE event.

Fig. 8. (a) Calculated LOED of four DFIGs (1.5, 2, 2.5 and 3 MW) at loading No. 14, (b) Calculated LOED of a 1.5 MW DFIG at light and heavy loading scenarios 1, 3, 4 and 6 during SPS, (c) FFT coefficients of the output active power for a 1.5 MW DFIG at loading No. 14 during SPS condition.

profile of output active power during the SPS condition for a 1.5 MW DFIG at loading No. 14. From this, it can be clearly seen that the FFT coefficients have increased at the low frequencies (0.3-7 Hz).

Also, Table 3 shows the calculated SPSD values of four DFIGs with pre-fault loading No. 14 following the SPS conditions. As expected in the SPS conditions, the FFT of output active power has a significant value in the low frequency coefficients. The results indicate that the SPSD is greater for larger DFIGs. In the next step, the results of a comparative test with regard to the various loading conditions for a 1.5 MW DFIG are discussed. As illustrated in Fig. 8 (b), after fault clearing at 8.2 s and during SPS condition, the calculated LOED values of all scenarios exceed the set threshold and it is worse for scenarios with leading power factor where DFIG absorbs a greater amount of reactive power. This result was expected be-

Table 3. SPSD of four DFIGs (1.5, 2, 2.5 and 3 MW) at loading No. 14 following SPS condition

DFIG rated power (MW)	SPSD (% of fundamental component)
1.5	27470
2	31268
2.5	44064
3	46092

Table 4. SPSD of a 1.5 MW DFIG at different loading scenarios

Scenario	SPSD (% of fundamental component)
1	9894
3	6582
4	103445
6	45382

cause in this mode of generator operation, the conventional LOE relays are more likely to maloperation [6]. Nevertheless, great SPSD values of all discussed scenarios in Table 3 show that the proposed method is independent of loading conditions. Concluding these results and other simulations, the B threshold value selected to be 1000. The results confirm that the proposed SPS detection method is applicable.

5. Conclusion

In this paper, a combined method is presented to detect the loss of excitation and to distinguish between stable power swing and the loss of excitation in the doubly fed

induction generator. The proposed LOE detection strategy is based on the multiplication of both the DFIG terminal voltage derivative and the DFIG output reactive power derivative, and the proposed SPS detection approach is defined using the sum of the low frequency range of the FFT coefficients of the DFIG three phase active power. The LOE detection method is corresponding to one of the newest articles published for the synchronous generators, developed here for the DFIG. Because this LOE detection method is prone to false operation during the SPS, an SPS detector is used in combination with the LOE detector herein. Using this solution, the LOE detection method has been promoted as well as removing the risk of incorrect operation. The proposed method was tested for several DFIG sizes under different loading conditions. The most important result of this paper is providing a LOE detection method for the DFIG as an innovation, while a strategy for fast SPS detection is proposed to prevent unwanted operation of the LOE relay. Therefore, the proposed method leads to more security and quickness.

Appendix

Parameters of the simulation model in Fig. 1

1. Parameters of 1.5-MW DFIG-based WT
   Vbase= 575 V; Sbase = 1.67 MVA; fbase = 60 Hz; ωs = 1 p.u.; ωb = 2 π fb = 377 rad/s; Rs = 0.00706 p.u.; Rr = 0.005 p.u.; Ls = 3.07 p.u.; Lr = 3.056 p.u.; Ls = 2.9 p.u.; Grid filter impedance: Rg + jXg = 0.003 + j 0.3 p.u.
2. Transmission lines parameters:
   Length: 30 km; Positive and zero sequence resistances: 0.1153, 0.413 Ω /km;
   Positive and zero sequence inductances: 1.05, 3.32 mH/km; Positive and zero sequence capacitances: 11.33, 5.01 nF/km;
3. Transformer parameters:
   T1 =2MVA, 575 V/25 KV, impedance: 0.0017 + j 0.05 p.u.; T2 =47MVA, 25 KV/120 KV,impedance: 0.00534 + j 0.16 p.u.
4. Network impedance:
   Re + jXe = 0.0004 + j 0.004 p.u.

References

[1] J., Yang. "*Fault analysis and protection for wind power generation systems*", Ph.D. dissertation, Dept. Electronics and Electrical. Eng., Univ. Glasgow, College of Science and Engineering, 2011.

[2] A., Khajeh and R., Ghazi, "*GA-Based Optimal LQR Controller to Improve LVRT Capability of DFIG Wind Turbines*", Iranian Journal of Electrical and Electronic Engineering, Vol. 9, No. 3, 2013.

[3] M., Zaggout, P., Tavner, C., Crabtree and Li., Ran, "*Detection of rotor electrical asymmetry in wind turbine doubly-fed induction generators*", IET Re-

newable Power Generation, Vol. 8, No. 8, pp. 878-886, 2014.

[4] M., Chen, L., Yu, N. S., Wade, X., Liu, Q., Liu and F., Yang, "*Investigation on the faulty state of DFIG in a microgrid*", IEEE Transactions on Power Electronics, Vol. 26, No. 7, pp. 1913-1919, 2011.

[5] A. P., Morais, G., Cardoso and L., Mariotto, "*An innovative loss-of-excitation protection based on the fuzzy inference mechanism*", IEEE Transaction on Power Delivery, Vol. 25, No. 4, pp. 2197-2204, 2010.

[6] M., Amini, M., Davarpanah and M., Sanaye-Pasand, "*A novel approach to detect the synchronous generator loss of excitation*", IEEE Transaction on Power Delivery, Vol. 30, No. 3, pp. 1429-1438, 2015.

[7] C. R., Mason, "*New loss-of-excitation relay for synchronous generators*", AIEE Transaction, Vol. 68, No. 2, pp. 1240–1245, 1949.

[8] J., Berdy, "*Loss of excitation protection for modern synchronous generators*", IEEE Transactions on Power Apparatus and Systems, Vol. 94, No. 5, pp. 1457–1463, 1975.

[9] IEEE Std. C37.102. IEEE Guide for AC Generator Protection, New York, 2006.

[10] E., Pajuelo, R., Gokaraju and M. S., Sachdev, "*Identification of generator loss-of-excitation from power-swing conditions using a fast pattern classification method*", IET Gen., Transm. Distrib., Vol. 7, No. 1, pp. 24–36, 2013.

[11] T., Amraee, "*Loss-of-field detection in synchronous generators using decision tree technique*", IET Generation, Transmission & Distribution, Vol. 7, No. 9, pp. 943–954, 2013.

[12] H., Yaghobi, "*Impact of static synchronous compensator on flux-based synchronous generator loss of excitation protection*", IET Generation, Transmission & Distribution, Vol. 9, No. 9, pp. 874–883, 2015.

[13] H., Yaghobi and H., Mortazavi, "*A novel method to prevent incorrect operation of synchronous generator loss of excitation relay during and after different external faults*", International Transactions on Electrical Energy Systems, Vol. 25, No. 9, pp. 1717-1735, 2015.

[14] H., Yaghobi and H., Mortazavi, "*Study on application of flux linkage of synchronous generator for loss of excitation detection*", International Transactions on Electrical Energy Systems, Vol. 23, No. 6, pp. 802-817, 2013.

[15] H., Yaghobi and H., Mortazavi, "*A novel flux-based method for synchronous generator loss of excitation protection*", Proc. of the 25th Int. Power System Conf., Tehran, Iran, pp. 1–14, 2010.

[16] A. F., Abdou, A., Abu-Siada and H. R., Pota, "*Ap-plication of STATCOM to improve the LVRT of DFIG during RSC fire-through fault*", In Universities Power Engineering Conference (AUPEC), 22nd Australasian, pp.1-6, 2012.

[17] A. F., Abdou, A., Abu-Siada and H. R., Pota, "*Improving fault ride through capability of DFIG during RSC flashover fault*", In Smart Energy Grid Engineering (SEGE), 2013 IEEE International Conference on, pp.1-5, 2013.

[18] J., Ouyang and X., Xiong, "*Dynamic behavior of the excitation circuit of a doubly-fed induction generator under a symmetrical voltage drop*", International Journal on Renewable Energy, Vol. 71, pp. 629-638, 2014.

[19] M., Hosseinabadi and H., Rastegar, "*DFIG Based Wind Turbines Behavior Improvement during Wind Variations using Fractional Order Control Systems*", Iranian Journal of Electrical and Electronic Engineering, Vol. 10, No. 4, 2014.

[20] F. K. A., Lima, A., Luna, P., Rodriguez, E. H., Watanabe and F., Blaabjerg, "*Rotor voltage dynamics in the doubly fed induction generator during grid faults*", IEEE Transactions on Power Electronics, Vol. 25, No. 1, pp. 118-130, 2010.

[21] W., Qiao, G. K., Venayagamoorthy and R. G., Harley, "*Real-Time Implementation of a STATCOM on a wind farm equipped with doubly fed induction generators*", IEEE transactions on industry applications, Vol. 45, No. 1, pp. 98-107, 2009.

[22] SimPowerSystems for use with Simulink. The Math Works, User's Guide, U.S.A., 2002.

[23] J., Mohammadi, S., Vaez-Zadeh, S., Afsharnia and E., Daryabeigi, "*A combined vector and direct power control for DFIG-based wind turbines*", IEEE Transactions on Sustainable Energy, Vol. 5, No. 3, pp. 767-775, 2014.

[24] R. J., Konopinski, P., Vijayan and V., Ajjarapu, "*Extended reactive capability of DFIG wind parks for enhanced system performance*", IEEE Transactions on power systems, Vol. 24, No. 3, pp. 1346-1355, 2009.

[25] B., Mahamedi and J., Zhu, "*A novel approach to detect symmetrical faults occurring during power swings by using frequency components of instantaneous three-phase active power*", IEEE Transaction on Power Delivery, Vol. 27, No. 3, pp. 1368–1375, 2012.

Mohammad javad Abbasi was born in Ilam, Iran, in 1989. He received his B.Sc. degree in Electrical Engineering from Kermanshah University of Technology in 2012, Kermanshah, Iran, and M.Sc. degree in Electrical Engineering from Semnan university in 2015, Semnan, Iran.

Hamid Yaghobi was born in Sari, Iran on 1978. He received his B.Sc. degree in Electrical Engineering from K.N.Toosi University of Technology in 2000, Tehran, Iran, M.Sc degree in Electrical Engineering from Ferdowsi University in 2002, Mashhad, Iran and his Ph.D. in electric machinery from the Department of Electrical Engineering of Ferdowsi University, Mashhad, Iran in 2011. He is currently an Assistant Professor at Semnan University. His research interests are modeling and fault diagnosis, design and protection of electrical machines.